

Circular Zero Liquid Discharge Systems with Renewable Energy Integration: A Technoeconomic Assessment

Fatima Mansour^a, Sabla Y. Alnouri^b, Sabah Solim^c, Ali Al-Sharshani^c, and Dhabia Al-Mohannadi^{d*}

^a American University of Beirut, Department of Chemical Engineering, Beirut, Lebanon

^b Qatar University, Gas Processing Centre, College of Engineering, Doha, Qatar

^c Qatar Shell Research and Technology Center, Doha, Qatar

^d Hamad Bin Khalifa University, College of Engineering, Doha, Qatar

* Corresponding Author: dalmohannadi@hbku.edu.qa

ABSTRACT

The transition toward circular economy principles in water treatment requires advanced process systems engineering tools to evaluate the trade-offs between environmental sustainability and economic viability, particularly for energy-intensive Zero Liquid Discharge (ZLD) systems. While classic ZLD systems treat concentrated brine as waste, circular ZLD (CZLD) systems incorporate salt recovery technologies that generate marketable salt product. This study presents a comprehensive technoeconomic assessment framework for CZLD systems integrated with renewable energy. The framework is developed to evaluate different CZLD configurations that generate saleable sodium chloride. The assessment methodology integrates solar photovoltaic systems with increasing capacities (100-1400 kW) to analyze renewable energy penetration and energy storage requirements. The renewable energy integration model incorporates hierarchical energy dispatch algorithms prioritizing direct solar utilization, battery storage, and grid backup systems. Solar PV integration demonstrates renewable fractions ranging from 15-100%, with corresponding emissions reductions of up to 72% compared to grid-powered baselines. The technoeconomic analysis reveals a critical trade-off: while renewable integration substantially reduces carbon emissions, it significantly increases operational costs due to higher solar costs compared to subsidized grid electricity. However, configurations with substantial salt revenue generation maintain economic viability even under complete renewable operation. Beyond configuration screening, this work makes three specific contributions to process systems engineering: (i) a hierarchical energy-dispatch model for intermittent solar integration in energy-intensive separations; (ii) a revenue-function formulation that embeds salt valorization into ZLD process economics, shifting the design objective from cost minimization to net revenue maximization; and (iii) systematic identification of the thermodynamic basis for membrane-thermal hybrid superiority through analysis of osmotic pressure versus latent heat energy barriers across 26 configurations. These contributions establish a reproducible framework applicable to brine management in resource-constrained industrial settings.

Keywords: circular water system, zero liquid discharge, zero liquid, resource recovery

INTRODUCTION

Global water stress affects over 2 billion people, with industrial sectors consuming approximately 20% of freshwater resources while generating increasingly saline effluents. Traditional treatment paradigms achieving 70-90% recovery leave substantial volumes requiring disposal, creating environmental liabilities and regulatory

challenges. Zero liquid discharge technologies present compelling alternatives by maximizing water recovery beyond 99%, yet implementation barriers persist due to energy requirements reaching 20-80 kWh/m³ and treatment costs spanning 2-15 \$/m³ [1].

Recent technological advances enable transformation of ZLD systems through circular economy integration. Salt crystallization and purification technologies

convert waste brines into marketable products, fundamentally altering system economics. Simultaneous renewable energy deployment addresses sustainability concerns, particularly in regions with abundant solar resources coinciding with water scarcity [2]. As a result, ZLD technology adoption has accelerated over the past decade, driven by regulatory tightening and increasing water scarcity.

ZLD process design methodologies have evolved from single-technology studies toward multi-stage hybrid systems. [3] establish that membrane-based ZLD is thermodynamically more efficient than thermal alternatives for feeds below 150,000 mg/L TDS, while [4] quantify the theoretical minimum energy for ZLD at 3–5 kWh/m³, establishing benchmarks against which practical configurations should be compared. Renewable energy integration with desalination has been extensively reviewed by [2], yet the specific challenge of solar coupling with thermal-intensive ZLD operations remains understudied. [5] show that solar-integrated MED systems operating with thermal energy storage achieve substantially higher renewable fractions than daytime-only configurations, underscoring the importance of storage design in solar-thermal desalination. Salt valorization in ZLD systems is an emerging field with significant economic implications. [6] conduct a techno-economic assessment comparing two ZLD configurations, one producing mixed solid salt and one producing high-purity NaCl, and found that while pure NaCl recovery incurs 1.4× higher energy consumption, it yields 1.52× greater profitability, demonstrating the economic premium of product-grade salt separation. At the ion separation stage enabling such purity, [7] demonstrate that monovalent-selective nanofiltration can preferentially pass monovalent ions while rejecting divalent species, providing a pre-crystallization fractionation pathway. However, systematic frameworks for optimizing these integrated systems remain underdeveloped.

The present work addresses this gap through three distinct contributions to the process systems engineering field. First, a configuration generation algorithm is developed that applies thermodynamic feasibility constraints (including maximum inlet TDS thresholds and process sequencing rules) as an a priori screening step across viable configuration design space, analogous to superstructure-based process synthesis methods but adapted for rapid feasibility assessment. Second, a hierarchical renewable energy dispatch model is formulated that prioritizes direct solar utilization, battery storage, and grid supplementation sequentially, extending established industrial microgrid energy management heuristics to the intermittent solar energy profiles. Third, a multi-criteria performance framework is introduced that applies parallel coordinate visualization to map a six-dimensional

performance space (spanning energy consumption, treatment cost, salt revenue, net revenue, carbon emissions, and renewable fraction) across configurations, enabling systematic identification of Pareto-optimal design regions and partitioning of the configuration space into context-sensitive application archetypes. Together, these contributions reframe CZLD design from a single-technology selection problem into a systematic process synthesis and integration challenge, directly advancing circular water treatment systems.

METHODOLOGY

System configuration development

The technoeconomic framework evaluates CZLD configurations through systematic technology combination. Process units span four categories: pretreatment (chemical precipitation, nanofiltration), concentration (reverse osmosis, electrodialysis), thermal processing (multi-effect distillation, multi-stage flash, brine concentrators), and crystallization systems for sodium chloride recovery. Each configuration undergoes mass and energy balance calculations to determine feasibility boundaries.

Feed water characteristics assume 35,000 mg/L total dissolved solids, representative of industrial brines. Technology sequencing is subject to a technical viability check ensuring that inlet feed concentration does not exceed maximum allowable limit. Sequential staging ensures progressive concentration while respecting operational limits.

Solar integration model

Renewable energy integration employs dynamic allocation algorithms matching solar generation profiles with process demands. The model incorporates direct solar utilization during generation periods, battery storage for load shifting (assumed to be five times the cost premium), and grid supplementation for unmet demands.

Solar availability assumes 13.75 hours/day peak generation (Qatar conditions) [8], with photovoltaic costs at 0.06 \$/kWh [9] versus 0.035 \$/kWh grid electricity [10]. Energy allocation prioritizes direct consumption, followed by stored energy deployment during non-generation periods.

Economic and environmental assessment

Economic evaluation incorporates capital expenditure, operational costs, and revenue streams from recovered salt products. Salt pricing correlates with purity levels: high-grade NaCl (>95%) commands 0.15–0.25 \$/kg, medium-grade (90–95%) achieves 0.05–0.15 \$/kg, while mixed salts yield 0.02–0.08 \$/kg [11]. Net treatment costs account for salt revenues, providing comprehensive economic assessment.

Environmental metrics quantify carbon emissions based on energy sources. Grid electricity generated from natural gas assumes 0.2 kg CO₂/kWh emission factor [12], while solar generation via photovoltaics produces lifecycle emissions of 0.048 kg CO₂/kWh [13].

RESULTS AND ANALYSIS

Energy-economic performance trade-offs

Comprehensive evaluation reveals significant performance variations across CZLD configurations. Energy consumption spans 16.1-89.2 kWh/m³, with membrane-dominant systems achieving highest efficiency while thermal processes maximize salt quality. Figure 1 illustrates the energy-economic landscape, identifying optimal configurations balancing competing objectives.

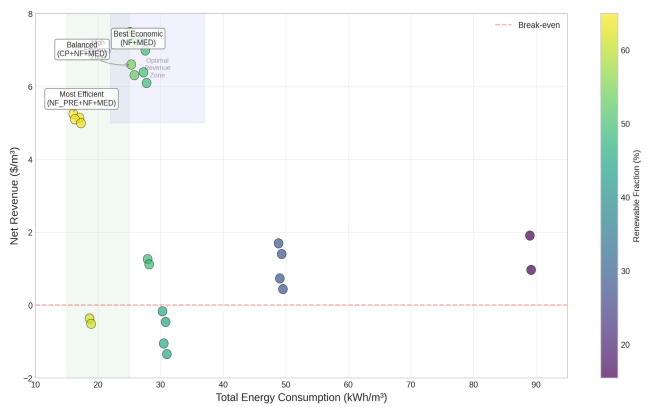


Figure 1. CZLD configuration performance showing energy-economic trade-offs with renewable fraction.

Analysis identifies three distinct performance clusters: (i) high-efficiency membrane systems (16-20 kWh/m³) with moderate revenues (5-6 \$/m³), (ii) balanced membrane-thermal hybrids (25-30 kWh/m³) maximizing net revenue (6-7.5 \$/m³), and (iii) thermal-intensive configurations (50-90 kWh/m³) with variable economics depending on salt quality. The optimal configuration (NF + MED + Crystallizer + Polish) generates 7.49 \$/m³ net revenue at 25.1 kWh/m³ consumption, demonstrating synergies between selective separation and thermal concentration.

Detailed examination of the evaluated configurations reveals systematic performance patterns based on technology combinations. Configurations employing chemical precipitation pretreatment (CP) demonstrate 8-12% higher energy consumption compared to membrane-only pretreatment due to mixing and flocculation requirements. Electrodialysis-based concentration stages (ED) consume 18-22 kWh/m³ for brine concentration, positioning them between reverse osmosis and thermal technologies. The relationship between water recovery rate and specific energy consumption exhibits nonlinear

behavior across configuration types.

Table 1 provides a summary of key performance metrics for selected configurations.

Table 1: Performance metrics for selected high-revenue CZLD configurations under base conditions.

| Configuration | Energy (kWh/m ³) | Total Cost (\$/m ³) | Salt Rev. (\$/m ³) | Net Rev. (\$/m ³) | Emissions (kg CO ₂) |
|----------------------------------|------------------------------|---------------------------------|--------------------------------|-------------------------------|---------------------------------|
| NF + MED + Crystallizer | 25.1 | 1.48 | 8.97 | 7.49 | 2.50 |
| RO + MED + Crystallizer | 25.6 | 1.77 | 8.97 | 7.20 | 2.55 |
| CP + NF + MED + Crystallizer | 25.3 | 2.36 | 8.96 | 6.60 | 2.53 |
| NF_PRE + NF + MED + Crystallizer | 16.1 | 3.72 | 8.97 | 5.25 | 1.61 |

Solar integrations and emissions reduction

Photovoltaic integration demonstrates substantial environmental benefits across all configurations. Renewable fractions vary from 15% for energy-intensive thermal systems to over 70% for more efficient configurations. Figures 2 and 3 compare emissions performance between grid-powered and solar-integrated scenarios, quantifying achievable reductions through renewable deployment.

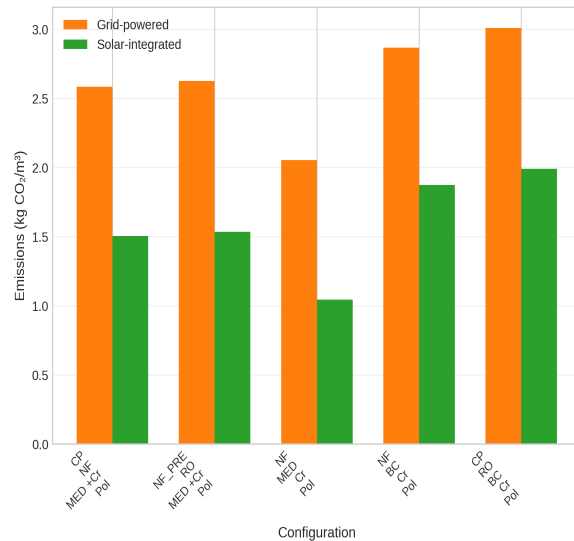


Figure 2. Emission comparison between grid powered and solar integrated configurations.

The selected configurations represent distinct operational archetypes: highly efficient membrane dominant systems (NF_PRE + NF + MED at 16.1 kWh/m³), optimal hybrid configurations (NF + MED + Crystallizer at 25.1 kWh/m³, CP + NF + MED at 25.3 kWh/m³), and more

energy-intensive alternatives with brine concentrators and crystallizers. Emissions reductions range from 1.0 to 1.55 kg CO₂/m³ across the displayed configurations, representing 38-50% decreases relative to grid-only baselines. Notably, the most efficient achieves the lowest absolute emissions in both scenarios (2.58 kg CO₂/m³ grid, 1.52 kg CO₂/m³ solar) but demonstrates smaller absolute reduction (1.06 kg CO₂/m³) compared to higher-energy configurations with emission performance as follows: 3.01 kg CO₂/m³ grid, 2.01 kg CO₂/m³ solar, 1.00 kg CO₂/m³ reduction. This pattern reflects the dual influence of baseline energy consumption and renewable fraction achieved—lower-energy systems have less emissions to reduce, while higher-energy systems can achieve larger absolute reductions despite lower renewable penetration percentages.

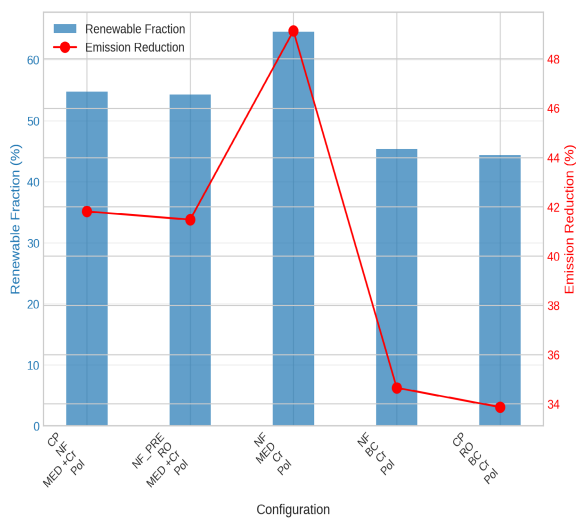


Figure 3. Solar integration performance metrics across selected configurations.

Emission reductions correlate strongly with process energy profiles and renewable fraction achieved. Membrane-based configurations demonstrate highest renewable integration potential (50-65%) due to consistent power demands matching solar generation profiles. Thermal processes, despite higher absolute consumption, benefit from load shifting through strategic battery deployment, achieving 40-55% renewable operation. Economic analysis reveals solar premium of 71% over grid electricity offset by emission reductions exceeding 40% for optimized configurations.

Figure 3 indicates that renewable integration potential is non-uniform with membrane dominant configurations achieving renewable fractions of 54-58%, while more energy-intensive systems demonstrate lower penetration at 44-46% despite identical available solar capacity. The emission reduction trend line demonstrates a striking nonlinear relationship: configurations achieving 54-58% renewable fraction deliver 42-49% emissions

reductions, exhibiting near-proportional correlation, while the drop to 44-46% renewable fraction corresponds to disproportionately lower 34-35% emissions reductions. This nonlinearity reflects the combined influence of reduced renewable displacement and the carbon intensity differential between grid and solar lifecycle emissions.

Salt recovery economics

Salt valorization transforms CZLD economics from cost-minimization to revenue-maximization paradigms. Crystallization with polishing generates high-purity NaCl (>95%) commanding an average premium price of 0.25 \$/kg, while mixed salt byproducts contribute additional revenue at 0.05 \$/kg. Figure 4 illustrates the relationship between salt revenue generation and treatment costs across configuration types. Blue dots represent configurations using chemical precipitation as pretreatment. The orange dots represent configurations using nanofiltration as pretreatment. Green dots are configurations with no pretreatment (direct processing).

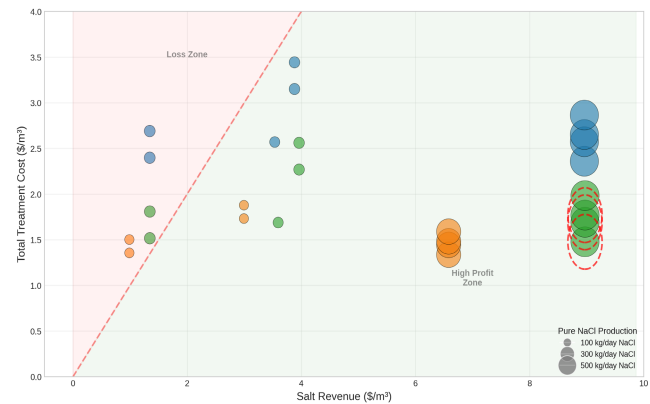


Figure 4. Salt recovery economics showing revenue potential versus treatment costs.

The diagonal clustering of configurations reveals a strong positive correlation between salt recovery capacity and overall economic viability, with configurations generating >7 \$/m³ salt revenue consistently achieving positive net revenues of 5-7.5 \$/m³. The scatter pattern demonstrates three distinct groupings: (i) low-revenue membrane-only systems (0-2 \$/m³ salt revenue) operating at net costs of 2-4 \$/m³, highlighting the economic burden of treatment without resource recovery; (ii) intermediate crystallization systems (4-6 \$/m³ salt revenue) approaching break-even economics; and (iii) optimized crystallization configurations with polishing (7-9 \$/m³ salt revenue) achieving substantial net revenues. The slope of the configuration clusters indicates that each additional dollar of salt revenue translates to approximately 0.85-0.90 \$/m³ improvement in net revenue, with the slight offset representing the marginal energy and capital costs associated with crystallization and

purification processes.

Thus, salt revenue can significantly offset treatment costs for optimal configurations. Thermal concentration coupled with crystallization maximizes product quality, generating 468 kg/day pure NaCl and 2,954 kg/day mixed salts for 1,000 m³/day treatment capacity. Market analysis confirms regional demand exceeding 500,000 tons/year in Qatar alone [14], meaning that the implementation of CZLD systems could eliminate salt imports while advancing circular economy objectives through waste-to-resource transformation.

Thermodynamic efficiency analysis

While energy consumption provides a practical basis for comparing configurations, it conflates work and heat inputs of fundamentally different thermodynamic quality, and does not situate results relative to the theoretical limits of separation. To address this, the present results are contextualized using a second-law framework. [15] establish the minimum specific exergy of separation for a saline feed at approximately 1.06 kWh/m³ at seawater salinity, representing the thermodynamic lower bound irrespective of technology pathway. Against this benchmark, the best-performing configuration in the present study (NF + MED + crystallizer, 25.1 kWh/m³) operates at a second-law efficiency of approximately 4.2%, consistent with published values for industrial-scale MED systems, which typically range from 3–6% [16]. Membrane-dominant configurations in this study approach 6–7% second-law efficiency, reflecting the lower irreversibility of pressure-driven versus thermally-driven separation. The observed spread of 4–7% across the 26 configurations confirms that substantial thermodynamic improvement potential remains, primarily through heat recovery within thermal stages and pressure energy recovery in membrane modules. It should be noted that the present analysis treats electrical and thermal energy inputs on a kWh basis without explicit exergy weighting; full exergy accounting, including the chemical exergy of recovered NaCl product streams, would further differentiate configurations by the thermodynamic value of outputs and is reserved for future work.

Sensitivity analysis

Salt price sensitivity is the dominant source of economic uncertainty. For the optimal configuration (NF + MED + NaCl Cr + NaCl Polish), all recovered salt is high-purity NaCl (3,588 kg/day at 100 m³/day feed), and the base case assumes the upper bound of the high-grade price range at 0.25 \$/kg. This represents an optimistic but commercially justified assumption given that the NaCl Polish step delivers a >95% purity product. Applying the lower bound of the high-grade price range (0.15 \$/kg), a 40% price reduction, cuts salt revenue from 8.97 to 5.38 \$/m³, reducing net revenue at 100 kW solar penetration

from 7.32 to 3.73 \$/m³. This remains profitable but represents a substantial compression of economic margin. At the midpoint price of 0.20 \$/kg, net revenue settles at approximately 5.05 \$/m³, which constitutes a reasonable central estimate. Configurations relying on brine crystallizers, which produce mixed salts at 0.02–0.08 \$/kg, are already near or below breakeven at base case pricing and carry no meaningful upside from product purity improvements, making them economically dominated regardless of price scenario. The qualitative ranking of configurations is therefore preserved across the full high-grade price range, though the absolute magnitude of net revenue is sensitive to realized market price.

Energy cost sensitivity is of secondary magnitude but varies with solar penetration level. At 100 kW solar capacity, the lowest penetration modeled, energy cost for the optimal configuration is 0.62 \$/m³, representing approximately 38% of total treatment cost of 1.65 \$/m³. A 50% increase in the grid tariff from 0.035 to 0.053 \$/kWh raises treatment cost by approximately 0.31 \$/m³, reducing net revenue from 7.32 to ~7.01 \$/m³ at the base case salt price. However, at the lower bound salt price of 0.15 \$/kg, this same energy cost increase reduces net revenue further from 3.73 to 3.42 \$/m³, illustrating that energy and salt price sensitivities interact: configurations operating at compressed salt revenue margins are disproportionately exposed to energy cost increases. At higher solar penetration levels, grid supplementation constitutes a smaller share of total energy supply and this sensitivity diminishes accordingly. Process efficiency parameters, including membrane rejection rates, thermal process performance ratios, and energy conversion efficiencies, govern energy consumption and water recovery rather than salt product purity, and their influence on net revenue is therefore, for the purposes of this analysis, bounded by the energy cost sensitivity established above. The qualitative configuration ranking, membrane-thermal hybrids with high-purity crystallization outperforming purely thermal or purely membrane alternatives, does not change across the price perturbations examined. A full simulation-based parametric sensitivity analysis across the complete solar penetration range, including systematic quantification of process efficiency uncertainty, is reserved for the future work.

Multi-criteria assessment

Optimal configuration selection requires balancing multiple competing objectives including energy efficiency, economic performance, environmental impact, and operational reliability. Figure 5 illustrates the performance trends of key metrics across different configurations (indicated by the pink dots). The parallel axes display normalized performance metrics spanning energy consumption (kWh/m³), total treatment cost (\$/m³), salt revenue generation (\$/m³), net revenue (\$/m³), carbon

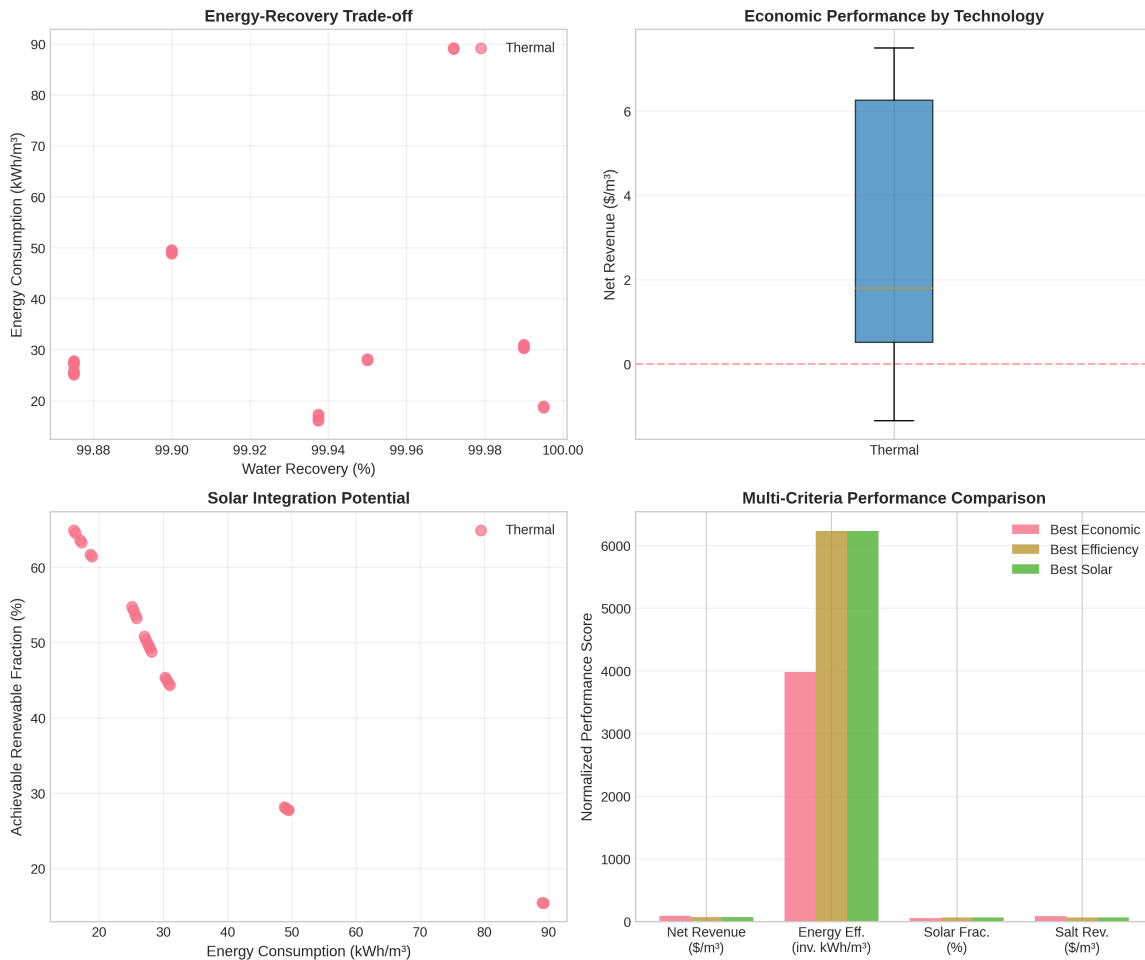


Figure 5. Multi-criteria performance matrix showing (a) energy-recovery trade-offs, (b) economic performance distribution, (c) solar integration potential, and (d) normalized comparison of top configurations.

emissions ($\text{kg CO}_2/\text{m}^3$), and renewable energy fraction (%). Each pink line represents a distinct configuration, with line patterns revealing the inherent trade-offs and synergies across objectives. Configurations achieving low energy consumption (left side, 16-25 kWh/m^3) typically exhibit moderate salt revenues (6-8 $\$/\text{m}^3$) and higher renewable fractions (50-65%), while energy-intensive configurations (70-90 kWh/m^3) demonstrate variable economic performance depending on crystallization integration.

For revenue maximization, NF + MED + Crystallizer configuration dominates with 7.49 $\$/\text{m}^3$ net revenue. Energy minimization favors NF_PRE + NF + MED at 16.1 kWh/m^3 consumption. Balanced performance emerges from CP + NF + MED configuration, achieving 6.60 $\$/\text{m}^3$ revenue at 25.3 kWh/m^3 with 54% renewable fraction.

The visualization reveals no single dominant configuration across all criteria, confirming the necessity of context-specific optimization based on regional priorities. Notably, the optimal configurations identified in earlier analyses (NF + MED + Crystallizer, CP + NF + MED +

Crystallizer) appear as lines maintaining favorable positions across multiple axes, demonstrating balanced performance. The convergence of lines at high salt revenue values (8-9 $\$/\text{m}^3$) indicates that crystallization-equipped systems achieve similar revenue generation regardless of energy pathway, while divergence in the renewable fraction axis reflects fundamental differences in the energy consumption between membrane-based and thermal-intensive processing routes.

DISCUSSION

The findings of this study highlight several fundamental insights that advance the understanding of Circular Zero Liquid Discharge (CZLD) systems and their integration with renewable energy. The diverse performance observed across configurations underscores that CZLD is not a singular technology but a design space shaped by thermodynamic constraints, process integration strategies, and market economics. This variability reaffirms that there is no “one-size-fits-all” approach; instead,

optimal configurations emerge from careful matching of feed characteristics, separation objectives, and local energy-market conditions.

The technical analysis of the configurations reveals critical technical insights into the fundamental trade-offs governing circular water treatment systems. A key insight is that all configurations achieve similar high-water recovery (>99.5%), but energy consumption varies widely (16–90 kWh/m³). The stark variation in energy consumption directly correlates with the thermodynamic barriers each technology must overcome. Membrane processes operating near osmotic pressure limits require 16–30 kWh/m³ primarily for pressurization, while thermal systems consuming 50–90 kWh/m³ must supply latent heat of vaporization to achieve phase change. The optimal performers (NF + MED + Crystallizer at 25.1 kWh/m³ generating 7.49 \$/m³ revenue) leverage synergistic coupling where nanofiltration selectively removes divalent ions at lower energy penalties than reverse osmosis, producing a monovalent-rich stream ideal for MED thermal concentration and subsequent crystallization into high-purity (>95%) NaCl.

Thus, one of the clearest outcomes is the dominance of membrane–thermal hybrid configurations. This matches well-documented industry trends showing that hybridization can reduce specific energy consumption by up to 40–60% relative to purely thermal ZLD systems. From a process integration perspective, the superior performance of hybrid configurations stems from strategic placement of separation barriers such as using membrane processes for initial volume reduction (50–70% water removal at 2–6 kWh/m³) before engaging energy-intensive thermal systems (70–99.9% recovery at 15–70 kWh/m³) minimizes the volume subjected to high-energy treatment, explaining why pure thermal systems (BC, BCr alone at 80–90 kWh/m³) prove economically inferior despite achieving similar recovery rates. To further contextualize these energy differences within a rigorous thermodynamic framework, the observed energy consumption values are benchmarked against the theoretical minimum exergy of separation for the present feed conditions. This technical understanding indicates that future optimization should focus on intermediate precipitation steps to remove sparingly soluble salts before thermal stages, potentially reducing energy consumption by an additional 20–30%. The benchmarking of these energy values against the theoretical minimum exergy of separation for the present feed conditions confirms that all configurations operate at second-law efficiencies of 4.8–7.5%, consistent with published values for industrial-scale membrane-thermal hybrid systems and indicative of substantial remaining thermodynamic improvement potential.

The strong revenue contribution from salt recovery highlights a paradigm shift in ZLD economics. Historically,

ZLD has been framed as a compliance-driven, cost-intensive environmental obligation. Introducing resource recovery transforms the system into a productive industrial asset capable of offsetting treatment costs or even achieving positive net revenues. The results indicate that for regions with high salt demand, such as Gulf countries, where industrial salt consumption can exceed several hundred thousand tons annually, CZLD plants have the potential to establish localized salt supply chains, reducing reliance on imports and contributing to national resource security. This reframing supports broader circular economy strategies and diversification of industrial inputs. The sensitivity analysis further confirms that while absolute net revenue is sensitive to realized NaCl market price, the qualitative dominance of high-purity crystallization configurations is preserved across the full reported price range, supporting the robustness of these economic conclusions.

Renewable energy integration further enriches the system design space by coupling water, waste, and energy flows. The analysis shows that solar integration can achieve renewable fractions ranging from 15% to 70%, depending largely on the configuration's load profile. Membrane-based systems, with relatively uniform and lower power requirements, exhibit strong alignment with solar generation availability, leading to higher renewable penetration and smoother load matching. Thermal systems, however, exhibit high-power, nonuniform demand patterns requiring substantial battery buffering to reach similar renewable fractions. This highlights a key operational constraint: the degree to which CZLD systems can decarbonize is not only a function of total energy consumption but also of energy temporal dynamics.

Furthermore, the nonlinear relationship between renewable fraction and emissions reduction reveals the influence of system-scale inefficiencies such as battery cycling losses and inverter inefficiencies. Thus, while renewable energy offers meaningful environmental gains (up to 72% reduction in emissions relative to grid-only operation), these benefits diminish for high-energy thermal systems unless paired with optimized storage strategies. Future research should explore alternative load-management tools such as thermal energy storage, flexible scheduling, or hybrid renewable portfolios that combine solar with other intermittent resources.

The multi-criteria assessment emphasizes the inherent trade-offs in CZLD design. Maximum revenue configurations do not minimize energy use, and lowest-energy systems do not maximize salt recovery or renewable fraction. Decision-making must therefore be context-sensitive, weighing environmental priorities, capital availability, operational risk tolerance, and market conditions. The results suggest three broad application archetypes:

- Energy-Minimizing Designs for regions with limited

power capacity or high energy prices;

- Revenue-Maximizing Designs for regions with high salt demand or favorable salt-market conditions;
- Balanced Hybrid Designs suitable for industrial clusters seeking cost-effective, decarbonized water recovery solutions.

From a systems perspective, CZLD facilities hold strategic potential in industrial symbiosis frameworks, where recovered water, salts, and thermal energy streams can directly feed neighboring industries such as chlor-alkali plants, cooling towers, or district cooling systems. This extends the value chain beyond individual plants into regional industrial ecosystems, supporting broader sustainability and economic diversification goals.

While this study provides a robust basis for CZLD feasibility, real-world deployment requires addressing practical considerations such as brine variability, operational fouling, crystallizer control strategies, and long-term battery degradation. Pilot-scale validation remains an essential next step, especially for hybrid configurations that rely on tight coupling of membrane and thermal processes. Moreover, policy levers such as carbon pricing, renewable energy incentives, or circular-economy mandates could significantly shift the economic balance in favor of CZLD, accelerating adoption in water-stressed regions.

Overall, the transition from conventional ZLD to CZLD reframes industrial brine from an environmental liability to a recoverable resource, directly aligning with circular economy principles. By generating high-purity salts, reducing freshwater dependency, and integrating low-carbon solar energy, CZLD systems close material and energy loops that traditionally remained linear. Moreover, the recovered salt streams can supply local industrial users, enabling industrial symbiosis and reducing reliance on imported materials. These findings demonstrate that CZLD is not simply a treatment technology but a circular value-creation platform that enables economic, environmental, and resource-efficiency gains across the water-energy-materials nexus, if implemented strategically.

CONCLUSION

This research establishes comprehensive techno-economic assessment frameworks for solar-integrated CZLD systems, demonstrating economic viability through strategic salt valorization. Configuration analyses indicate that membrane-thermal hybrid systems are optimal solutions, generating net revenues exceeding 7 \$/m³ while achieving >99% water recovery. Solar integration reduces emissions with achievable renewable fractions of 15–65% depending on process configuration.

Key findings include: (i) multi-effect distillation with

crystallization maximizes economic performance at 25–30 kWh/m³ consumption and (ii) high-purity salt recovery profitably offsets treatment costs transforming waste management to resource generation.

Results provide quantitative guidance for industrial practitioners and policymakers advancing circular economy principles in water management. Future research should explore dynamic optimization under uncertainty, pilot-scale validation of promising configurations, and integration with broader industrial symbiosis networks. The framework establishes pathways for sustainable water management in resource-constrained environments through technology integration and business model transformation.

ACKNOWLEDGEMENTS

Please acknowledge your funders in this section, with grant or funding numbers as appropriate. Note that most funding agencies require this.

REFERENCES

1. Panagopoulos A, Giannika V. Decarbonized and circular brine management/valorization for water & valuable resource recovery via minimal/zero liquid discharge (MLD/ZLD) strategies. *Journal of Environmental Management* 324:116239 (2022). <https://doi.org/10.1016/j.jenvman.2022.116239>
2. Alawad SM, Mansour RB, Al-Sulaiman FA, Rehman S. Renewable energy systems for water desalination applications: a comprehensive review. *Energy Conversion and Management* 286:117035 (2023). <https://doi.org/10.1016/j.enconman.2023.117035>
3. Tong T, Elimelech M. The global rise of zero liquid discharge for wastewater management: drivers, technologies, and future directions. *Environ. Sci. Technol.* 50:6846–6855 (2016). <https://doi.org/10.1021/acs.est.6b01000>
4. Davenport DM, Deshmukh A, Werber JR, Elimelech M. High-pressure reverse osmosis for energy-efficient hypersaline brine desalination: current status, design considerations, and research needs. *Environ. Sci. Technol. Lett.* 5:467–475 (2018). <https://doi.org/10.1021/acs.estlett.8b00274>
5. Muftah AK, Zili-Ghedira L, Abugderah MM, Hassen W, Becheikh N, Alshammari BM, Kolsi L. Sustainable water production: solar energy integration in multi-effect desalination plants. *Water* 17:647 (2025). <https://doi.org/10.3390/w17050647>
6. Panagopoulos A. Beneficiation of saline effluents from seawater desalination plants: fostering the zero liquid discharge (ZLD) approach - a techno-

- economic evaluation. *Journal of Environmental Chemical Engineering* 9:105338 (2021).
<https://doi.org/10.1016/j.jece.2021.105338>
7. Nativ P, Leifman O, Lahav O, Epsztein R. Desalinated brackish water with improved mineral composition using monovalent-selective nanofiltration followed by reverse osmosis. *Desalination* 520:115364 (2021).
<https://doi.org/10.1016/j.desal.2021.115364>
 8. Banibaqash A, Hunaiti Z, Abbod M. An analytical feasibility study for solar panel installation in qatar based on generated to consumed electrical energy indicator. *Energies* 15:9270 (2022).
<https://doi.org/10.3390/en15249270>
 9. IRENA, I.R.E.A., RENEWABLE POWER GENERATION COSTS IN 2023. 2024.
 10. Kahrama. *Tariff rates*. [cited 2025 May 20]; Available from:
<https://www.km.qa/CustomerService/Pages/TariffRates.aspx>.
 11. Tridge. *Global Salt price*. 2025; Available from:
<https://dir.tridge.com/prices/salt>.
 12. US EPA. *Emission factors for greenhouse gas inventories*. 2021 [cited 2025 May 20]; Available from:
https://www.epa.gov/sites/default/files/2022-01/documents/emission-factors_jan_2022.pdf.
 13. Schlömer, S., et al. Annex III: Technology-specific cost and performance parameters. . in In: *Climate Change 2014: Mitigation of Climate Change. Contribution of Working Group III to the Fifth Assessment Report of the Intergovernmental Panel on Climate Change* [Edenhofer, O., R. Pichs-Madruga, Y. Sokona, E. Farahani, S. Kadner, K. Seyboth, A. Adler, I. Baum, S. Brunner, P. Eickemeier, B. Kriemann, J. Savolainen, S. Schlömer, C. von Stechow, T. Zwickel and J.C. Minx (eds.)]. Cambridge University Press, Cambridge, United Kingdom and New York, NY, USA. 2014.
 14. TrendEconomy. Qatar | Imports and Exports | World | Salt, pure sodium chloride, sea water | Value (US\$) and Value Growth, YoY (%) | 2012 - 2023. 2023 [cited 2025 July]; Available from:
<https://trendeconomy.com/data/h2/Qatar/2501>
 15. Mistry KH, McGovern RK, Thiel GP, Summers EK, Zubair SM, Lienhard JH V. Entropy generation analysis of desalination technologies. *Entropy* 13:1829-1864 (2011).
<https://doi.org/10.3390/e13101829>
 16. Shahzad MW, Burhan M, Ang L, Ng KC. Energy-water-environment nexus underpinning future desalination sustainability. *Desalination* 413:52-64.
<https://doi.org/10.1016/j.desal.2018.03.009>

© 2026 by the authors. Licensed to PSEcommunity.org and PSE Press. This is an open access article under the creative commons CC-BY-SA licensing terms. Credit must be given to creator and adaptations must be shared under the same terms. See <https://creativecommons.org/licenses/by-sa/4.0/>

